

Supporting Information

Photoinitiated Growth of Sub-7 nm Silver Nanowires within a Chemically Active Organic Nanotubular Template

D. M. Eisele¹, H. v. Berlepsch², C. Böttcher², K. J. Stevenson³,

D. A. Vanden Bout^{3,1}, S. Kirstein¹, J. P. Rabe^{*,1}

¹*Humboldt-Universität zu Berlin, Institut für Physik, Newtonstr. 15, 12489 Berlin, Germany,*

²*Freie Universität Berlin, Institut für Chemie und Biochemie, Research Centre for Electron Microscopy,*

Fabeckstr. 36a, 14295 Berlin, Germany,

³*The University of Texas at Austin, Department of Biochemistry and Chemistry and Center*

for Nano and Molecular Science and Technology, Austin, Texas 78712, USA

Contents

1. CryoTEM and HR-TEM of silver nanostructures	S2
1.1. Diameter of the silver nanowire and the template	S2
1.2. Polycrystalline silver nanowire	S3
1.3. Silver growth process on and within the template	S5
1.4. Silver wire with partially removed template	S6
2. UV-Vis absorption upon exposure to white light	S7
3. Materials and methods	S8

1. CryoTEM and HR-TEM of silver nanostructures

1.1 Diameter of the silver nanowire and the template

The diameter of the silver nanowire was taken from the line profile normal to the nanowire shown in **Figure 3a** of the manuscript. **Figure S1a** shows this line profile averaged 145 nm along the nanowire. The full width at half maximum (FWHM) was taken as the diameter of the silver nanowire and is (6.4 ± 0.5) nm. The variation of the diameter along the nanowire was investigated by taking several line profiles each averaged over 15 nm along the nanowire. The variations in the diameter were found to be within the error of ± 0.5 nm as shown in **Figure S1b**. It is noted here that after longer reaction times homogeneous nanowires have been found in the solution as well with slightly increased diameter.

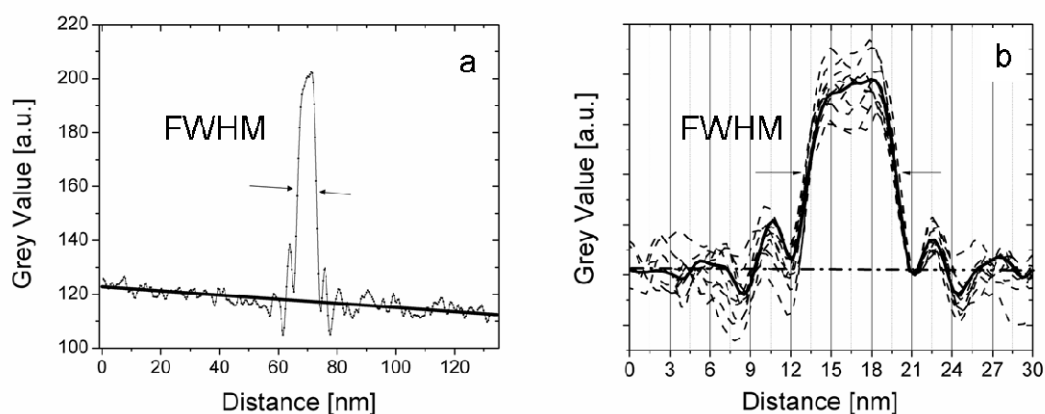


Figure S1: Line scans across silver nanowire shown in Figure 3; (a) line scan averaged over 145 nm along the nanowire, (b) several line profiles each averaged 15 nm along the nanowire.

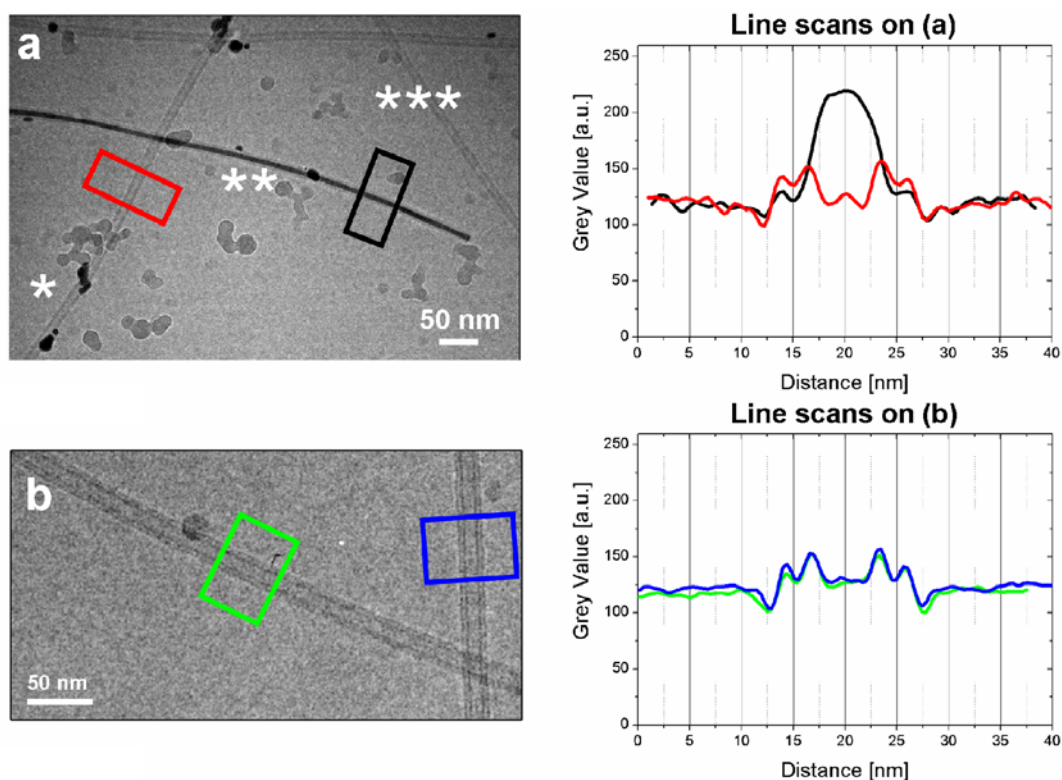


Figure S2: CryoTEM of the vitrified J-aggregate solution with/without AgNO_3 : **(a)** Representative CryoTEM images of a frozen sample prepared from a solution 15 min after adding AgNO_3 and exposing it to white light for 20 s. Line scans taken on the empty template (red box = red solid line) and on the filled template (black box = black solid line) reveal no significant changes of the templates' diameter upon filling with silver. **(b)** CryoTEM of neat J-aggregate solution (no AgNO_3). Line scans taken on the empty template (green, blue box = green, blue solid line, respectively) reveal no significant changes of the templates' diameter compared to (a).

1.2 Polycrystalline silver nanowire

Figures S3 a, b show representative HR-TEM images of an illuminated J-aggregate/ AgNO_3 solution dried on a TEM grid and examined within a day. The nanowires exhibit a polycrystalline structure. Contrasts variation along the nanowire are observed, which are attributed to the different orientations and sizes of the crystallites.

The distance between the periodic minima of the grey values in **Figure S3 a, c** is $d = (0.237 \pm 0.002)$ nm. The error has been determined by averaging d from different HR-TEM images. In **Figure S3 b, d** the ABC stacking of a fcc crystal, including twinning,^{i,ii} can be observed. The lattice structures shown in **Figures S3** are attributed to the Ag(111) planes of the fcc crystal of Ag. The increased diameter of the wires is attributed to thickening during the preparation for TEM imaging.

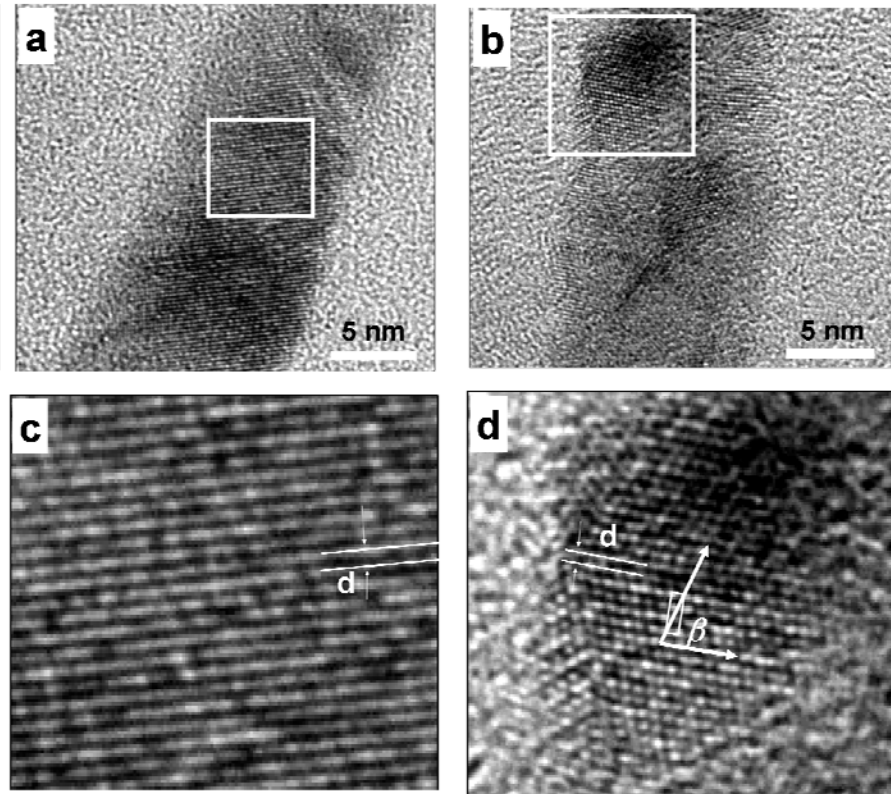


Figure S3: HR-TEM images of a nanowire section. The J-aggregate solution containing AgNO_3 was exposed to white light for 90 min, transferred and dried on a TEM grid and probed with a day. **(a),(b)** The silver nanowire shows a polycrystalline structure; **(c)** magnified from (a) shows a periodic lattice structure with $d = (0.237 \pm 0.002)$ nm, which can be assigned to the distance between Ag(111) planes; **(d)** magnified from (b) with stacking and twinning assigned to the fcc structure of Ag with $\beta = (69 \pm 3)^\circ$ and $d = (0.235 \pm 0.002)$ nm.

1.3 Silver growth process on and within the template

CryoTEM and TEM images like shown in **Figure 3** of the manuscript that the redox reaction on the exterior of the nanotubular template leads to the growth of isolated silver seeds rather than covering the whole nanotube with many small silver nanoparticles. The silver growth process inside of the nanotubular template might be different than on the outside.

The schematic displayed in **Figure S4** shows two possible growth processes for silver nanostructures (in black) on the interior of the nanotubular template (in red). **Figure S4 a** shows a scheme in which the nanotube's interior is covered at first by many small silver seeds, so that the growth process may lead to regions where the tube is not completely filled with silver. **Figure S4 b** depicts a scheme in which the growth process is similar to that found on the tube's exterior, in which isolated silver seeds are growing until they completely fill the interior of the tubular template.

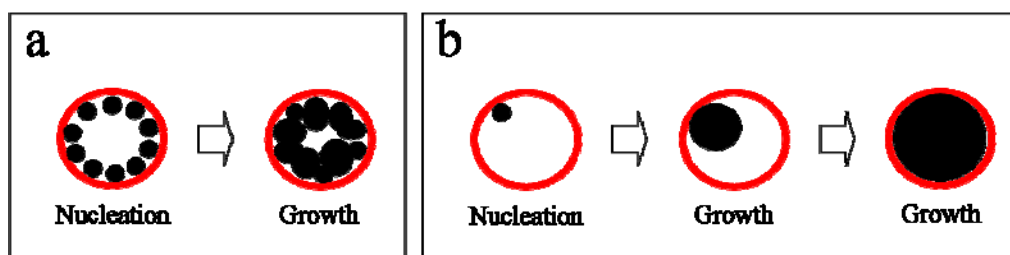


Figure S4: Schematic illustrates the silver growth (black) inside the tubular template (red): the two possibilities (a) and (b) are detailed in the text.

The images shown in **Figure S3** clearly demonstrate that the silver nanowires are compact rather than tubular, and composed of crystalline regions nearly as large as the diameter of the template. Therefore, HR-TEM and CryoTEM images suggest a similar growth process on and within the template as depicted in **Figure S4 b**.

1.4 Silver wire with partially removed template

It was previously shown that upon diluting the neat J-aggregate solution with methanol the J-bands absorption was decreased while the monomer absorption increases.ⁱⁱⁱ This makes methanol an excellent candidate for removing the J-aggregate template from the silver nanowires upon rinsing the solution with it. **Figure S5** shows a cryo-TEM image of a solution containing silver nanowires after rinsing the solution with methanol where it can be seen that the template was partially removed from the silver wire.

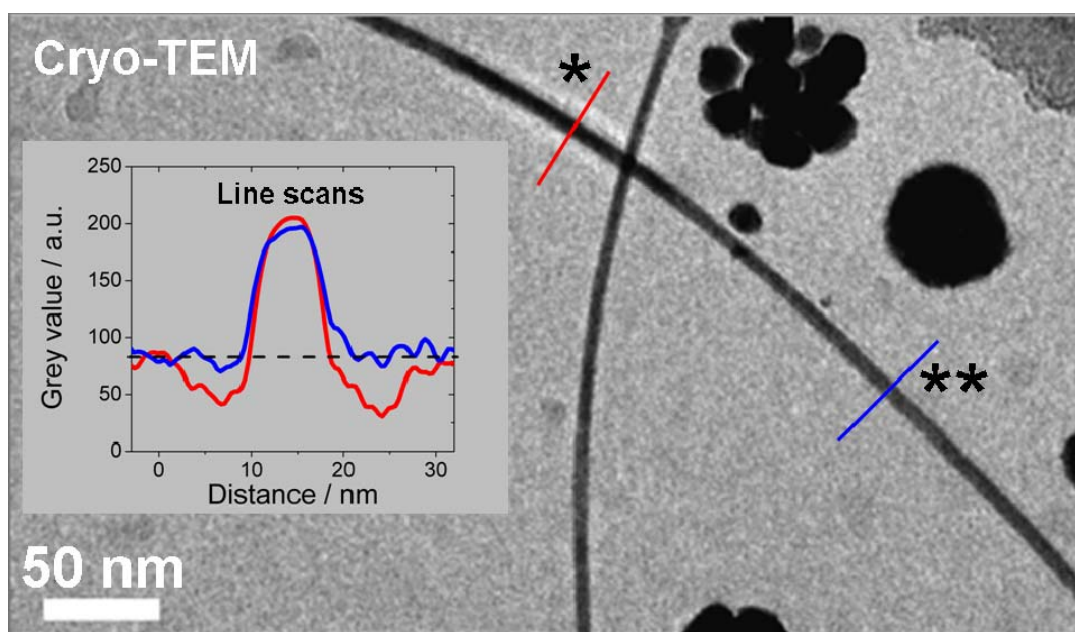


Figure S5: CryoTEM image of a frozen sample prepared from tubular J-aggregate solution 72h after adding AgNO_3 , exposing it to white light for 90 min., and rinsing the solution with 50% methanol: (*) tubular J-aggregate filled with silver wire and (**) silver wire with partially removed template, see also line scans for demonstration that by rinsing with methanol the organic template could be partially removed from the silver wire.

2. UV-Vis Absorption upon exposure to white light

The silver nanowire growth in the interior of the tubular template is photoinitiated. Evidence that the silver nanostructure growth is light enhanced and continues after the illumination is stopped, is provided by monitoring the changes in the absorption spectra in the UV-Vis range shown in **Figure 2** in the manuscript and on **Figure S6**.

The spectral changes within the first 45 min after preparation and exposure to white light for 5 min are shown in **Figure S6**. The spectra show the initial illumination step (5 min) leads to only a small loss in absorption, followed by further oxidation of the template in the absence of light.

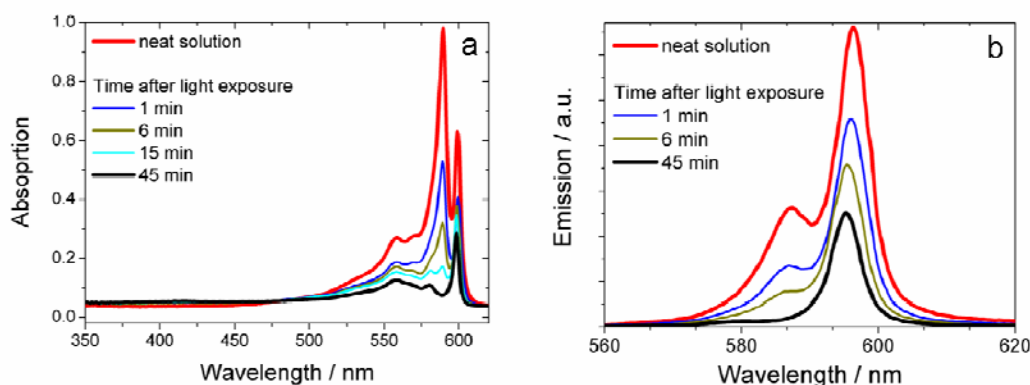


Figure S6: (a) Absorption and (b) emission spectra of J-aggregate solution with AgNO_3 . Red: Pure J-aggregate solution. Absorption and emission after the first 45 min after adding AgNO_3 and exposure to white light for 5 min. decrease continuously towards the final trace (black).

3. Materials and methods

Preparation of nanotubular J-aggregates

The amphiphilic cyanine dye derivative 3,3'-bis(2-sulfopropyl)-5,5',6,6'-tetrachloro-1,1'-dioctylbenzimidacarbocyanine (C8S3, MW = 902.8 g/mol, was obtained as a sodium salt (FEW Chemicals, Wolfen, Germany) and used as received. Double-walled nanotubular J-aggregates were prepared as described in detail elsewhere.^{iv}

Preparation of silver nanostructures

To a 400 ml C8S3 J-aggregate solution 11 ml 100 mM AgNO₃ solution was added. The solution was illuminated with a white light fluorescent bulb at different exposure times for 20 s up to 90 min.

Absorption spectroscopy

Absorption spectra from the solution were taken with a double-beam UV-Vis spectrometer (Shimadzu UV-2101PC) in a 0.1 mm/0.2 mm demountable quartz cell (Hellmar GmbH, Germany).

Cryogenic Transmission Electron Microscopy (CryoTEM)

Droplets of the solution (5 µL) were applied to perforated (1 µm hole diameter) carbon film covered 200 mesh grids (R1/4 batch of Quantifoil Micro Tools GmbH, Jena, Germany), which had been hydrophilized before use by simply storing the grids over a water bath for a day. The supernatant fluid was removed with a filter paper until an ultra-thin layer of the sample solution was obtained spanning the holes of the carbon film. The samples were immediately vitrified by propelling the grids into liquid ethane at its freezing point (90 K) operating a guillotine-like plunging device.

Frozen samples were transferred into a Philips CM12 TEM using the Gatan cryo-holder and -transferstation (Model 626, Gatan Inc., USA). Microscopy was carried out at 94 K sample temperature using the microscopes low dose protocol at a calibrated primary magnification of 58 300x and an accelerating voltage of 100 kV (LaB6-illumination).

The defocus was chosen to be 1.2 μ in order to create sufficient phase contrast for imaging.

Image analysis was performed with WaveMetrics, Inc. software (IGOR Pro 6.0).

High Resolution Transmission Electron Microscopy (HR-TEM)

High resolution transmission electron microscopy (TEM) was performed with a JEOL 2010F operating at 200 kV.

Droplets of the solution (5 μ L) were applied to carbon film covered 200 mesh grids (Quantifoil Micro Tools GmbH, Jena, Germany), which had been hydrophilized before use by simply storing the grids over a water bath for a day. The supernatant fluid was removed with a filter paper until an ultra-thin layer of the sample solution was obtained on the carbon film.

Image analysis was performed with WaveMetrics, Inc. software (IGOR Pro 6.0).

Optical dark field microscopy

Optical dark field microscopy was performed using an optical microscope (Nikon Eclipse E600) using dark field condensor (Nikon Oil 1.43-1.20) and objective: Nikon, Plan Flour, 100x / 0.7-1.3 (Transmission mode). Images have been recorded by a CCD camera (CoolSNAP).

We note that dark field optical microscopy is an easy method, compared to (TEM or CryoTEM) to verify if there are long silver nanostructures within the solution. **Figure S7** shows a representative dark field optical microscopy image of J-aggregate solution with AgNO₃ after exposure to white light for 90 min and storing 2 months in the darkness. The solution is captured between two glass slides allowing the objects in the solution to move within the solution while imaging.

As expected, with dark field optical microscopy in the pure J-aggregate solution without AgNO₃ no tubular or wire like structures could be found. Only dimmer spots in the solution could be observed, likely from scattering signal of dust particles. Therefore

dimmer spots in **Figure S7** can be assigned either to the scattering signal of dust as found in the pure J-aggregate solution or to very small silver particles.

Objects causing brighter spots (higher contrast) could not be found in the pure J-aggregate solution and thus can be assigned to silver particles. The long objects that show homogenous scattering contrast along the long axis can be assigned to long silver nanostructures such as silver nanowires.

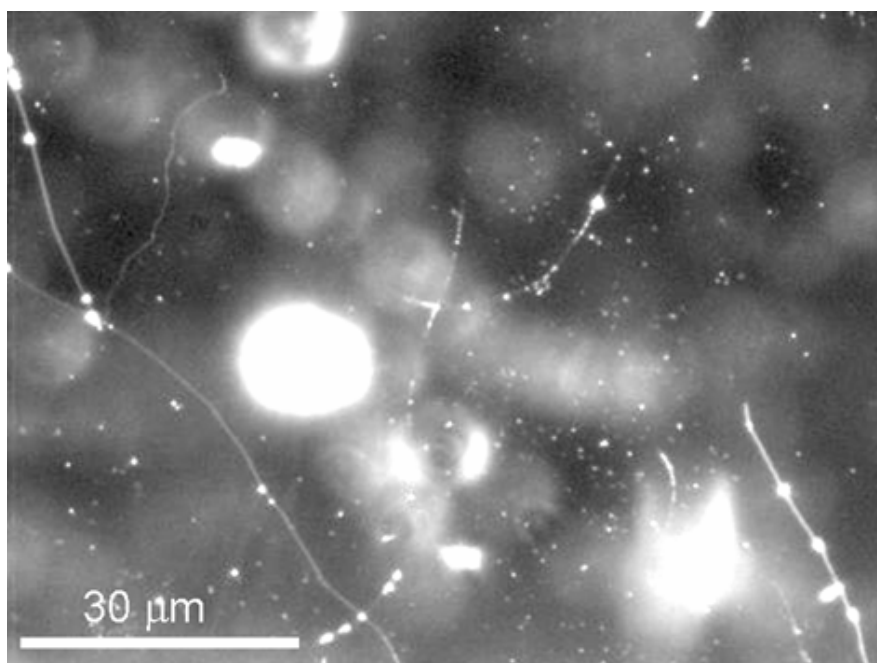


Figure S7: Dark field optical microscopy image J-aggregate solution with AgNO₃: non-dried J-aggregate solution 2 months after adding AgNO₃ and exposure to white light for 90 min, imaged at different focal planes; an optical microscope with 100x objective (NA 0.7-1.3) and dark field condensor was used.

ⁱ Charles Kittel, *Introduction to Solid State Physics*, 1986, John Wiley & Sons, Inc

ⁱⁱ Wang, J.; Tian, M.; Mallouk, T. E.; Chan, M. H. W. *J. Phys. Chem. B* **2004**, *108*, 841-845.

ⁱⁱⁱ von Berlepsch, H; Kirstein, S.; Hania, R.; Pugzlys, A.; Böttcher, C. *J. Phys. Chem. B* **2007**, *111*, 1701-1711.

^{iv} Lyon, J. L.; Eisele, D. M.; Kirstein, S.; Rabe, J. P.; Vanden Bout, D. A.; Stevenson, K. J. *J. Phys. Chem. C* **2008**, *112*, 1260-1268.